Diffusing Wave Spectroscopy Microrheology of Actin Filament Networks

Andre Palmer,* Thomas G. Mason,* Jingyuan Xu,* Scot C. Kuo,# and Denis Wirtz*
*Department of Chemical Engineering, The Johns Hopkins University, Baltimore, Maryland 21218, and #Department of Biomedical Engineering, The Johns Hopkins University, Baltimore, Maryland 21205 USA

ABSTRACT Filamentous actin (F-actin), one of the constituents of the cytoskeleton, is believed to be the most important participant in the motion and mechanical integrity of eukaryotic cells. Traditionally, the viscoelastic moduli of F-actin networks have been measured by imposing a small mechanical strain and quantifying the resulting stress. The magnitude of the viscoelastic moduli, their concentration dependence and strain dependence, as well as the viscoelastic nature (solid-like or liquid-like) of networks of uncross-linked F-actin, have been the subjects of debate. Although this paper helps to resolve the debate and establishes the extent of the linear regime of F-actin networks' rheology, we report novel measurements of the high-frequency behavior of networks of F-actin, using a noninvasive light-scattering based technique, diffusing wave spectroscopy (DWS). Because no external strain is applied, our optical assay generates measurements of the mechanical properties of F-actin networks that avoid many ambiguities inherent in mechanical measurements. We observe that the elastic modulus has a small magnitude, no strain dependence, and a weak concentration dependence. Therefore, F-actin alone is not sufficient to generate the elastic modulus necessary to sustain the structural rigidity of most cells or support new cellular protrusions. Unlike previous studies, our measurements show that the mechanical properties of F-actin are highly dependent on the frequency content of the deformation. We show that the loss modulus unexpectedly dominates the elastic modulus at high frequencies, which are key for fast transitions. Finally, the measured mean square displacement of the optical probes, which is also generated by DWS measurements, offers new insight into the local bending fluctuations of the individual actin filaments and shows how they generate enhanced dissipation at short time scales.

INTRODUCTION

Filamentous actin (F-actin), one of the constituents of the cytoskeleton, is believed to be one of the most important participants in the mechanical integrity of eukaryotic cells. The mechanism by which F-actin networks provide cells with structural rigidity is attributed to their viscoelastic nature, characterized by viscoelastic moduli.

However, major discrepancies between reported values of the magnitude of the viscoelastic moduli of uncross-linked F-actin networks, their concentration dependence, strain dependence, and frequency dependence have appeared in the literature. These vastly different rheological data have yielded different conclusions regarding the separate role of F-actin in the cell's structural rigidity. Traditionally, the linear viscoelastic moduli of F-actin networks in vitro have been investigated by imposing a mechanical strain and quantifying the resulting stress. Reported elastic moduli of uncross-linked F-actin networks, measured using mechanical deformation, differ by more than two orders of magnitude, between 10 and 40 dynes/cm^2 (Pollard et al., 1986; Sato et al., 1987; Wachstock et al., 1993) and 1000–5000 dynes/cm^2 (Hvidt and Heller, 1990; Janmey et al., 1990, 1991, 1994; Hvidt and Janmey, 1990). Therefore, concentrated F-actin solutions have been described as forming networks that are either weak or stiff (note: we use the terms "network" and "solution" interchangeably; both terms describe a semidilute solution of highly purified, uncross-linked F-actin). Furthermore, some researchers have reported that networks of uncross-linked F-actin harden for strains between 1% and 10% (Hvidt and Heller, 1990; Janmey et al., 1990, 1994), which corresponds to elastic moduli increasing with strain, and yield beyond 10%. In contrast, other researchers have not observed any strain-hardening effect, only the onset of yielding when the strain reaches 10% (Pollard et al., 1986; this work). Finally, vastly different values of the relative magnitudes of elastic and loss moduli, which characterize the nature of the viscoelasticity, have helped researchers to characterize F-actin networks as either viscoelastic solid or viscoelastic liquids.

The actual magnitude of the elastic modulus is important because a high value would support the hypothesis that isotropic F-actin networks alone are strong enough to stabilize cells (Janmey et al., 1994). A high value of the elastic modulus also provides a baseline against which to monitor subtle changes in the mechanical properties of F-actin networks due to regulating proteins such as capping and severing proteins, as well as small changes due to polymerization of actin filaments from ATP-containing or ADP-containing subunits (Newman et al., 1993; Pollard et al., 1986; Janmey et al., 1991). Finally, it supports the hypothesis that F-actin alone can effectively provide structural rigidity for the reinforcement of a new cellular protrusion (Condeelis, 1992).

The strain dependence of F-actin networks' rheology is also important: if F-actin networks strain-harden, they can potentially stabilize the cytoskeleton, even when it is subject to large deformations. Moreover, the strain dependence

Received for publication 30 April 1998 and in final form 19 October 1998.
Address reprint requests to Dr. Denis Wirtz, Department of Chemical Engineering, Johns Hopkins University, Maryland Hall, Room 221, 3400 North Charles Street, Baltimore, MD 21217. Tel.: 410-516-7006; Fax: 410-516-5510; E-mail: wirtz@jhu.edu.

0006-3495/99/02/1063/09 $2.00

of the viscoelastic moduli establishes the extent of the rheological linear regime (for which moduli are independent of strain), which is important because it allows for meaningful comparison with theoretical models and other mechanical measurements.

Given the controversy surrounding traditional methods, we have developed a novel, light-scattering-based technique, diffusing wave spectroscopy (DWS), which probes the linear rheological properties of biopolymer networks noninvasively (Palmer et al., 1998; Petka et al., 1998). This technique and associated analysis are based on the measurement of the autocorrelation function of the light multiply scattered from microspheres imbedded in the network. From the measured autocorrelation function and using a generalized Stokes-Einstein equation, we extract the mean square displacement of the probing microspheres. From these mean square displacements, we calculate the viscoelastic moduli of networks of highly purified, uncross-linked F-actin. This technique is somewhat similar to single particle tracking microrheology (SPTM), recently developed by Wirtz and co-workers (Mason et al., 1997a,b; Xu et al., 1998c; Ganesan et al., unpublished data) and Schmidt and co-workers (Schnurr et al., 1997a,b). Unlike SPTM, which monitors the displacement of a single particle at a time, DWS monitors many thousands of microspheres simultaneously, which allows for superior statistics. However, unlike DWS, SPTM allows us to probe the mechanical properties of an anisotropic F-actin specimen and the cytoskeleton of a living cell in situ (Ganesan et al., unpublished data).

Our optical rheometry assay generates measurements of the viscoelastic moduli of F-actin networks that are less ambiguous than mechanical measurements. In particular, this instrument exploits the small, random, thermally induced force generated by imbedded microspheres and therefore avoids possible flow-induced orientation and bundling of actin filaments. In the absence of externally applied forces, optical rheometry probes the viscoelastic properties of networks in the linear small-strain regime almost by definition. Moreover, this optical instrument greatly increases the frequency range of the probed viscoelastic moduli: we routinely probe frequency-dependent loss and elastic moduli at frequencies up to 1 MHz, which is four orders of magnitude larger than possible with mechanical rheometry. This extended range of frequency allows us to probe the internal dynamics of actin filaments in concentrated solutions as well as the effect of fast cellular transitions on F-actin rheology. Finally, the measured mean square displacement of the optical probes, which is also generated by DWS measurements, offers new insight into the local bending fluctuations of the individual actin filaments and shows how these generate large dissipation at short time scales.

EXPERIMENTAL TECHNIQUES

Actin preparation

Actin was purified from rabbit skeletal acetone powder by the method of Spudich and Watt (1971). The resulting actin was then gel filtered on Sephacryl S-300 HR instead of Sephadex G-150 (MacLean-Fletcher and Pollard, 1980). The purified actin was stored as Ca^{2+}-actin in continuous dialysis at 4°C against buffer G (0.2 mM ATP, 0.5 mM dithiothreitol, 0.1 mM $CaCl_2$, 1 mM sodium azide, and 2 mM Tris-Cl, pH 8.0). The final actin concentration was determined by ultraviolet absorbance at 290 nm, using an extinction coefficient of $2.66 \times 104\ M^{-1}\ cm^{-1}$ and a cell path length of 1 cm. Mg^{2+} actin filaments were generated by adding 0.1 volume of 10× KME (500 mM KCl, 10 mM $MgCl_2$, 10 mM EGTA, 100 mM imidazole, pH 7.0) polymerizing salt buffer solution to 0.9 volume of G-actin in buffer G. We did not observe large variations in the mechanical properties of F-actin networks measured by optical and mechanical rheometry on actin extracted and purified by the method of MacLean-Fletcher and Pollard (1980) and by the new method of Casella et al. (Casella and Torres, 1994; Casella et al., 1995). This new actin purification method includes an additional cycle of polymerization/depolymerization followed by an additional gel filtration step. We verified that G-actin, which is filtrated once, contained negligible amounts of capping proteins by monitoring the polymerization of actin, using time-resolved fluorescence spectroscopy and pyrene-labeled actin (not shown here). We also note that our actin samples were never frozen for storage purpose.

For this study, six actin concentrations ranging from 10 μM (0.42 mg/ml) to 164 μM (6.89 mg/ml) are reported. While uncross-linked F-actin solutions of concentrations smaller than ~48 μM are isotropic liquids, F-actin solutions of concentrations greater than 48 μM form a highly ordered liquid-crystalline phase (Coppin and Leavis, 1993): we report optically measured viscoelastic moduli of F-actin solutions in the liquid-crystalline phase and in the isotropic phase.

Diffusing wave spectroscopy

Instrument

The beam from an Ar^+ ion laser operating in the single-line frequency mode at a wavelength of 514 nm is focused and incident upon a flat scattering cell that contains the F-actin network and spherical optical probes. The light multiply scattered from the solution is collected by two photomultiplier tubes (PMTs) via a single-mode optical fiber with a collimator lens of very narrow angle of acceptance at its front end and a beamsplitter at its back end (Weitz and Pine, 1993). The outputs of the PMTs are directed to a correlator working in the pseudo-cross-correlation mode to generate the autocorrelation function $g_2(t) - 1$, from which quiescent rheological properties of the F-actin solutions can be calculated.

Actin is polymerized in situ for 12 h before measurement by loading the scattering cell with a solution of G-actin mixed with the polymerizing salt solution and a dilute suspension of monodisperse latex microspheres (Duke Scientific Corp.) of radius 0.48 μm at a volume fraction of 1%. The scattering cell is then immediately tightly capped. Using time-resolved mechanical rheology, we verified that G-actin was fully polymerized into F-actin and that F-actin had formed an equilibrium network at all concentrations presented in this paper before 12 h. Using mechanical rheology, we also verified that the rheology of F-actin is identical in the presence and in the absence of the added latex beads. Using static light scattering, we verified that more than 98% of the scattering intensity in the transmission geometry was due to the microspheres, and less than 2% was due to the F-actin filament network itself. We also verified that the measured mean square displacement scaled inversely with the radius of the probing bead for diameters larger than 0.55 μm and smaller than 1.95 μm (see Eq. 1 below). Smaller particles did not display saturation of their displacement at large times (they percolated through the network), and larger particles sedimented too rapidly (data not shown). All DWS measurements are conducted at a temperature of 23°C.

Analysis

The general method used to extract $G'(\omega)$ and $G''(\omega)$ from $g_2(t) - 1$ via the calculated values of the mean square displacement of the optical probes is described in Mason and Weitz (1995) and Palmer et al. (1998). The method

is based on a relation between the mean square displacement of a microsphere imbedded in a viscoelastic medium and the viscoelastic modulus of that medium. By assuming that Stokes' law, which holds for a purely viscous fluid, can be generalized to all frequencies, one obtains

$$\tilde{G}(s) = s\tilde{\eta}(s) \cong \frac{k_B T}{\pi a s \langle \Delta \tilde{r}^2(s) \rangle}, \quad (1)$$

where s is the Laplace frequency and $\tilde{}$ represents the unilateral Laplace transformation, defined as $\tilde{X}(s) \equiv L[X(t)] \equiv \int_0^\infty X(t)\exp(-st)dt$. Equation 1, which neglects inertial effects, relates the unilateral Laplace transforms of the stress relaxation modulus $G_r(t)$, $\tilde{G}(s) \equiv s\tilde{G}_r(s)$, and of the mean square displacement $\langle \Delta r^2(t) \rangle$. We use the analytic continuation between the real function $\tilde{G}(s)$ and the complex function $G^*(\omega) \equiv G'(\omega) + iG''(\omega)$ to extract elastic and loss moduli by extracting real and imaginary parts from the imaginary function $\tilde{G}(s = i\omega)$.

Mechanical rheometry

To compare our optical measurements with classical mechanical measurements (Ferry, 1980), we employ a strain-controlled mechanical rheometer (ARES-100 Rheometrics) equipped with a 50-mm-diameter cone-and-plate geometry. To prevent possible evaporation of the buffer, the cone-and-plate tools are enclosed in a custom-made vapor trap. The temperature of the sample is fixed at 23°C to within 0.1°C. The G-actin solution is placed between the cone-and-plate tools and allowed to polymerize in the presence of polymerizing salt for 12 h before the measurements. The viscoelastic properties of F-actin networks were found independently of time after 12 h at all actin concentrations used in this work. The linear equilibrium values $G'(\omega)$ and $G''(\omega)$ of the actin solutions are measured by setting the amplitude of the oscillatory strain at $\gamma = 1\%$ and sweeping from low to high frequency. The strain-dependent viscoelastic moduli were measured by subjecting the F-actin solution to a 1-rad/s oscillatory deformation of increasing amplitude; G' and G'' are computed from the maximum magnitude of the measured stress (Palmer et al., 1998; Mason et al., 1998).

RESULTS

Computation of the mechanical properties of F-actin networks from multiple light scattering measurements proceeds via several steps. We report the autocorrelation function $g_2(t) - 1$ of the multiply scattered light intensity, measured with a fast intensity correlator. From $g_2(t) - 1$, we compute the mean square displacement $\langle \Delta r^2(t) \rangle$ of the microspheres (for further details about how $\langle \Delta r^2(t) \rangle$ is calculated from $g_2(t) - 1$, see Weitz and Pine, 1993; Palmer et al., 1998), from which we extract the time-dependent diffusion constant $D(t)$. From $\langle \Delta r^2(t) \rangle$, we calculate the viscoelastic modulus $\tilde{G}(s)$, and finally the frequency-dependent viscoelastic moduli $G'(\omega)$ and $G''(\omega)$.

Correlation function, mean square displacement, and time-dependent diffusion coefficient

The light of an Ar^+ ion laser is incident upon the F-actin network and multiply scattered by the microbeads imbedded inside the network. We measure the instantaneous intensity of the light intensity multiply scattered by the microspheres, transmitted through the network, detected by the PMTs, and then autocorrelated to generate the autocorrelation function $g_2(t) - 1$. Fig. 1 shows $g_2(t) - 1$ over a large temporal range

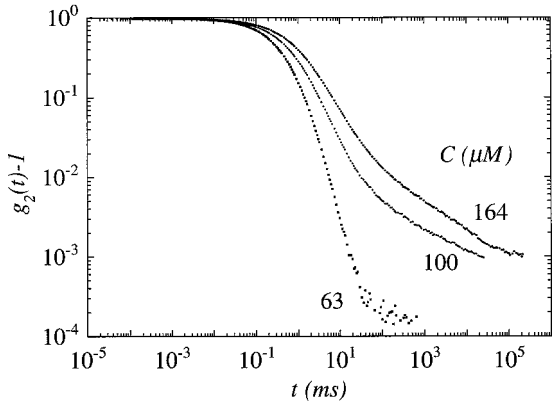

FIGURE 1 Autocorrelation function $g_2(t) - 1$ of the light intensity multiply scattered by 0.96-μm-diameter microspheres imbedded in actin filament networks. This scattered light is detected by the PMTs, and $g_2(t) - 1$ is calculated by the cross-correlator of the DWS instrument obtained after a 12-h run on F-actin networks. From these high-temporal-resolution measurements, we extract the mean square displacement, $\langle \Delta r^2(t) \rangle$. From these $\langle \Delta r^2(t) \rangle$ measurements, we calculate the viscoelastic moduli of F-actin networks.

corresponding to ~10 time decades, between 10^{-7} s and 10^3 s. By collecting at least four DWS runs for each actin concentration, we confirmed the reproducibility of our optical measurements of $g_2(t) - 1$. Sample aging effects are negligible; no significant optical and rheological changes occurred within 3–5 days after the preparation of G-actin and (immediate) subsequent polymerization for 12 h. At large actin concentration, problems from lack of ergodicity can arise because of the onset of inhomogeneities in F-actin networks. To confirm ergodicity, we conducted runs on the same F-actin samples with the laser beam incident upon five different points of the face of the scattering cell. Local variations of $g_2(t) - 1$ were found to be negligible for actin concentration smaller than 48 μM but observed to slightly increase for increasing actin concentration (data not shown).

From $g_2(t) - 1$ data, we extract the time-dependent mean-square displacement $\langle \Delta r^2(t) \rangle$ of the spherical probes imbedded in the mesh formed by the overlapping actin filaments. The result of this operation is displayed in Fig. 2, which shows that the motion of the probing spheres is rapid at short times and dramatically slowed past a characteristic time. The time at which probe motion becomes hindered is more rapidly attained for increasing actin concentrations, and, as expected, the maximum displacements reached by the diffusing microspheres decrease with actin concentration. Fig. 3 displays $\langle \Delta r^2(t) \rangle$ as a function of actin concentration and time scale. All graphs display a similar weak dependence on actin concentration. From $\langle \Delta r^2(t) \rangle$, we can also calculate the time-dependent diffusion coefficient $D(t) \equiv \langle \Delta r^2(t) \rangle / 6t$, which is shown in Fig. 4. As discussed below, this figure shows that the transport of microspheres with a diameter larger than the average mesh size is not purely diffusive and therefore is not characterized by a single constant diffusion coefficient, but by a time-dependent diffusion coefficient.

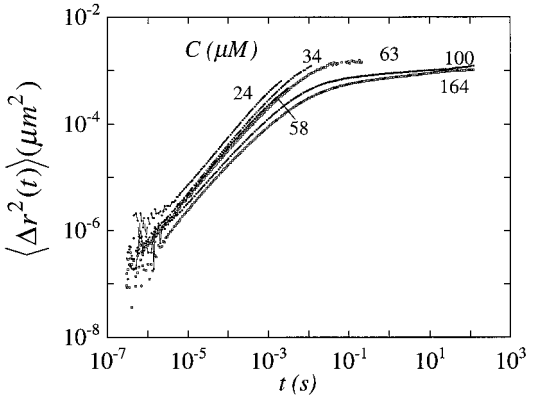

FIGURE 2 Time-dependent mean square displacement $\langle \Delta r^2(t) \rangle$ of the spherical probes imbedded in the mesh formed by the overlapping actin filaments extracted from $g_2(t) - 1$ data via a method detailed in Palmer et al. (1998). The motion of the probing spheres is rapid at short times and dramatically slowed past a characteristic time. The time at which probe motion becomes hindered is more rapidly attained for increasing actin concentrations, and, as expected, the maximum displacements reached by the diffusing microspheres decrease with actin concentration. The average radius of the probes is 0.48 μm.

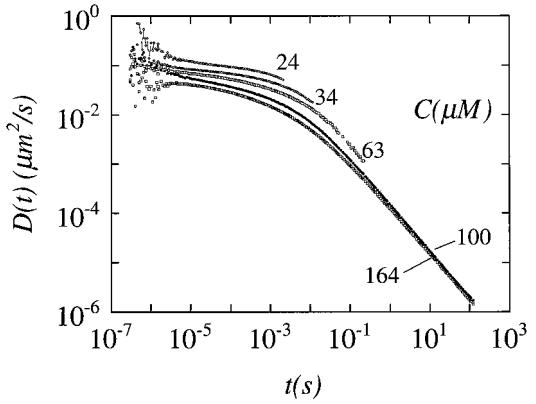

FIGURE 4 Time-dependent diffusion coefficient, defined as $D(t) \equiv \langle \Delta r^2(t) \rangle / 6t$, of the microspheres imbedded in the F-actin network. The diffusion constant D spans six orders of magnitude, from $D \approx 10^{-6}$ μm^2/s for large actin concentrations and long times to $D \approx 0.3$ μm^2/s for small actin concentrations and short times. As expected, this last value is on the order of magnitude of the diffusion coefficient of a sphere of radius $a = 0.48$ μm in water, which is a constant equal to $D_0 = k_B T/6\pi\eta a \approx 0.44$ μm^2/s.

Complex modulus

To extract the viscoelastic moduli of actin filament networks, we adapt the analytical framework developed in Mason and Weitz (1995). In particular, the macroscopic viscoelastic modulus $|\tilde{G}(s = i\omega)| = |G^*(\omega)| = \sqrt{G'^2(\omega) + G''^2(\omega)}$, which can be computed directly by Laplace transformation of the discrete $\langle \Delta r^2(t) \rangle$ data and is displayed in Fig. 5. Each curve displays a characteristic plateau at small frequencies up to a concentration-dependent characteristic crossover frequency and a rapid increase for increasing frequency after that crossover frequency.

We can also extract the concentration dependence of the high-frequency viscoelastic modulus. Fig. 6 displays $|G^*|$ measured at $\omega = 10^5$ rad/s as a function of actin concentration; a power-law fit of the data yields

$$|G^*| \propto c^{0.5}. \quad (2)$$

A simple model, offered by Maggs (personal communication), can explain the nontrivial concentration dependence of the high-frequency viscosity, $\eta_\infty \propto \sqrt{c}$. At short time scales, the bead moves relative to the background of immobile filaments. The hydrodynamic flow created by the moving bead is screened into the network and is nonnegligible up to a distance ξ into the sample from the bead. Thus dissipation per unit volume is $k_B T\dot{S} \approx \eta\nu^2/\xi^2$. Therefore, the total dissipation is on the order of $\sim\eta(\nu^2/\xi^2)(R^2\xi)$. But $\xi \propto c^{-1/2}$; hence the friction is proportional to $c^{1/2}R^2$, in qualitative agreement with our observations.

Elastic and loss moduli

Elastic and loss moduli are straightforwardly extracted from $\tilde{G}(s)$ because $G'(\omega) = |G^*(\omega)|\cos(\pi\alpha(\omega)/2)$ and $G''(\omega) = |G^*(\omega)|\sin(\pi\alpha(\omega)/2)$, where $G^*(\omega) = \tilde{G}(s = i\omega)$. The fre-

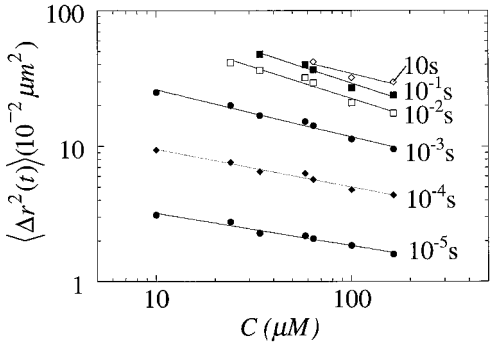

FIGURE 3 $\langle \Delta r^2(t) \rangle$ as a function of actin concentration at sampling times varying from $t = 10^{-5}$ s to $t = 10$ s.

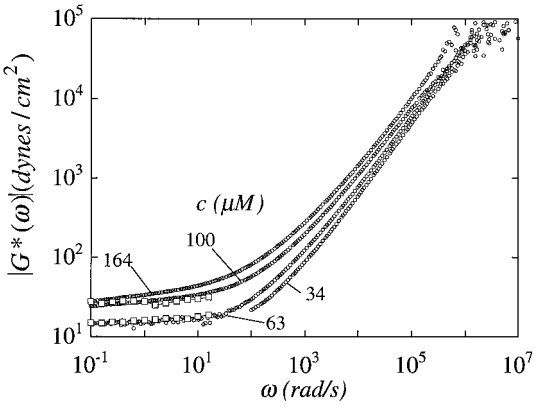

FIGURE 5 Complex viscoelastic modulus $|G^*(\omega)| = \sqrt{G'^2 + G''^2}$ as a function of the frequency obtained from $\langle \Delta r^2(t) \rangle$ data (see text for details).

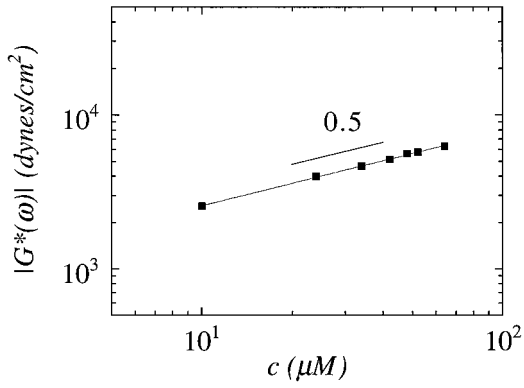

FIGURE 6 High-frequency viscoelastic modulus as a function of actin concentration. The fit of the data yields $|G^*| \propto \sqrt{c}$. The modulus is estimated at $\omega = 10^5$ rad/s.

quency-dependent phase shift $\alpha(\omega)$ determines the nature of the transport of the microspheres in the F-actin network. If $\alpha = 0$, the probed polymer network is purely elastic; if $\alpha = 1$, the network is purely dissipative. Fig. 7 shows the frequency-dependent elastic and loss moduli of a 24 μM F-actin network. Fig. 7 also shows $G'(\omega)$ and $G''(\omega)$ measured by mechanical rheometry. Excellent agreement is observed between optical and mechanical measurements over the limited frequency range probed by our mechanical rheometer. The elastic modulus G' is observed to dominate at low frequencies, and the loss modulus G'' dominates at large frequencies. We measure

$$G'(\omega) \propto G''(\omega) \propto \omega^{0.78\pm0.10} \quad \text{for } \omega > 200\ \text{s}^{-1} \qquad (3)$$

for a 24 μM F-actin network. As discussed below, the frequency dependence of $G''(\omega)$ as well as the dominance of $G''(\omega)$ at high frequency are unusual for a polymeric system.

In Fig. 8, we plot the low-frequency elastic plateau modulus G'_p, which is evaluated at $\omega = 1\ \text{s}^{-1}$ (i.e., $G'_p \approx G'(\omega = 1\ s^{-1})$), as a function of actin concentration c. For the sake

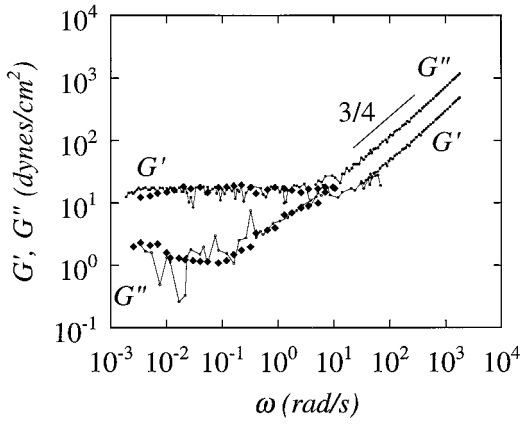

FIGURE 7 Elastic and loss moduli as measured by DWS of a 24 μM F-actin network. At low frequencies, F-actin networks are weak and solid-like. At high frequencies, F-actin networks are liquid-like; the loss modulus dominates the elastic modulus.

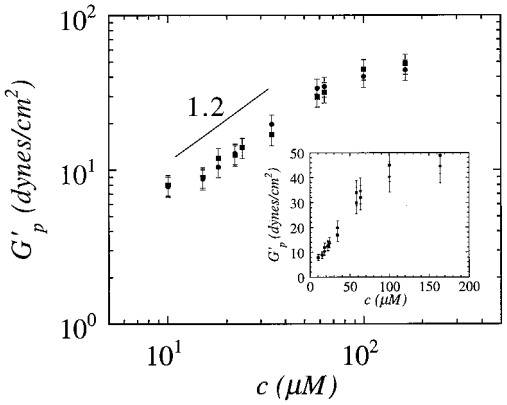

FIGURE 8 Low-frequency elastic modulus G'_p as a function of actin concentration. For the sake of comparison, we also plot $G'_p(c)$ as measured by mechanical rheometry. For concentration $c \leq 64$ μM, the data are fit by a power law of c; we find $G'_p(c) \propto c^{1.2\pm0.2}$. This figure shows saturation in the measured G'_p at concentration $c > 64$ μM, which may indicate the onset of local liquid crystalline order at high actin concentration.

of comparison, we also plot $G'_p(c)$ as measured by mechanical rheometry. For concentration $c \leq 60$ μM, the data are fit by a power law of c; we find

$$G'_p(c) \propto c^{1.2\pm0.2}. \qquad (4)$$

Fig. 8 also shows saturation of G'_p at concentrations $c > 60$ μM, which may indicate the onset of local liquid crystalline order at high actin concentration.

DISCUSSION

Fast bending modes at short times and hindered diffusion at long times

Our high-bandwidth measurements of the mean square displacement are sensitive to both the fast bending fluctuations of single actin filaments at short times and the macroscopic viscoelasticity of F-actin networks at long times. Morse's model (Morse, manuscript submitted for publication) predicts that the viscoelastic modulus of a concentrated network of F-actin is $G^*(\omega) \propto (i\omega)^{3/4}$ at large frequencies. Therefore, according to Eq. 1, $\langle \Delta r^2(t) \rangle \propto t^{3/4}$ at short times, in excellent agreement with our observations. This good agreement suggests that the exponent ¾ describes the fast bending fluctuations of the filaments at wavelengths shorter than the entanglement length of the network. This exponent is therefore directly related to the finite rigidity of individual actin filaments. At long times, the microspheres become elastically trapped by the actin filaments. The associated diffusion coefficient D of the probing 0.48-μm radius microsphere decreases from $D \approx 0.3$ μm^2/s at short times to $D \approx 10^{-6}$ μm^2/s for large actin concentrations and long times. The latter value corresponds to near-arrest of the microsphere by the elastic F-actin network: the microsphere probes the long-time elasticity of the F-actin mesh. The former is close but smaller than the diffusion coefficient of

the same microsphere in water of viscosity 1 cP, which is equal to $D_0 = k_B T/6\pi\eta a \approx 0.44\ \mu m^2/s$.

The values of D that we measured by DWS can be compared with values obtained by Newman and co-workers using classical dynamic light scattering (Newman et al., 1989a,b). These authors measured the diffusion coefficient of latex spheres imbedded in F-actin networks and obtained values ranging from $D/D_0 \approx 1$ to 0.2 for 270-nm-radius spheres in F-actin networks of concentrations ranging from 1 to 22 μM. The magnitudes of these values agree with our optical measurements, at least if we use D optically measured at very short times and small actin concentrations. But, as shown in Fig. 4, the diffusion of latex spheres in concentrated F-actin networks is not well described by a single, constant diffusion coefficient, because the spheres' transport becomes subdiffusive at times as short as 10^{-4} s. Indeed, we obtain values that are 10^5 to 10^6 smaller than D_0 at long times and large actin concentrations. The interpretation of Newman et al. (1989a) only incorporates the dissipative nature of the F-actin network (i.e., the viscosity) and does not include the elastic contribution to the hindered diffusion of the microsphere in the F-actin network.

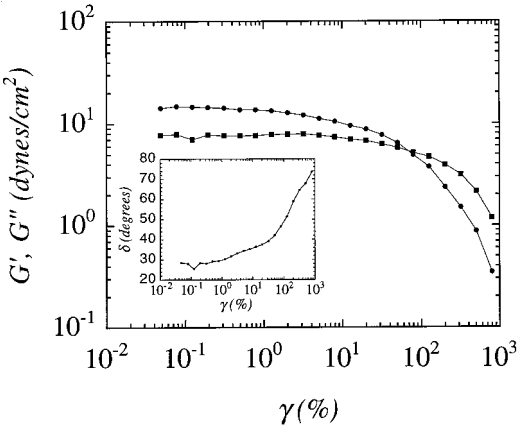

FIGURE 9 Loss and storage moduli of a 24 μM F-actin network as a function of strain. This figure shows that the rheology of F-actin networks does not display strain-hardening and that the linear regime extends up to strains of 10%. The inset shows that the shift angle δ between loss and storage modulus is a strong function of strain. At small strains, $\delta = 25°$, and an F-actin solution is a viscoelastic fluid with a solid-like character. At large strains, δ increases toward 90°, and an F-actin solution becomes a viscoelastic fluid with a liquid-like character.

Agreement between optical and mechanical measurements

Over the limited frequency range probed by mechanical rheometry, our mechanical and optical measurements agree to within 10–15% (see Fig. 7). This agreement between optical and mechanical measurements helps clarify the behavior of F-actin under deformation. Researchers have reported conflicting observations regarding the low-strain behavior of F-actin networks. In particular, Janmey et al. (1994) have reported strain-hardening. We have repeated these measurements with our instruments, and instead observe that G' and G'' are strain-independent for strains up to $\gamma \approx 10\%$ (see Fig. 9). Because we obtain the same magnitude for G' and G'' with mechanical rheometry (which involves shear deformation) and optical rheometry (which involves no applied shear deformation), we conclude that F-actin networks do not display strain-hardening and therefore do not offer a reserve of resistance to deformation.

Frequency dependence of viscoelastic moduli

The viscoelastic nature of F-actin networks strongly depends on the strain frequency

The description of F-actin rheology has been oversimplified. We find that the frequency content of mechanical deformation governs the viscoelastic response of an F-actin network. Because of the large variations in the reported values of their elasticity, uncross-linked F-actin networks have been characterized as either viscoelastic solids or viscoelastic liquids (Janmey et al., 1988, 1990, 1991, 1994; Sato et al., 1985, 1987). The extremely large temporal resolution of DWS allows us to show that the rheological behavior of F-actin networks can be characterized as both solid-like and liquid-like. At small frequencies, actin filament networks can be characterized as viscoelastic gels because they display some of the characteristic rheological properties of gels. These characteristics include an elastic modulus that is nearly frequency-independent over a wide frequency range and is much larger than the loss modulus (solid-like behavior). However, at small frequencies, uncross-linked F-actin networks are weak: the magnitude of the plateau modulus is small. Instead, at high frequencies, both elastic and loss moduli become large. Moreover, at high frequencies, F-actin networks are liquid-like: the loss modulus systematically dominates the elastic modulus and F-actin networks lose their solid-like properties.

Comparison with reported values and theoretical models

Rheological measurements of the frequency dependence of the elastic and loss moduli for $\omega > 100$ rad/s are not available in the literature; therefore direct comparison with published data is impossible. Moreover, like stress-controlled rheometers (Janmey et al., 1994), magnetic microrheometers (Schmidt et al., 1996; Muller et al., 1991), and torsion pendulums (Zaner, 1986; Janmey et al., 1994), our strain-controlled rheometer can measure $G'(\omega)$ and $G''(\omega)$ only up to 80–100 rad/s, so a direct comparison between DWS measurements and mechanical measurements at higher frequencies is also precluded.

However, recent theoretical models predict the high-frequency dependence of both $G'(\omega)$ and $G''(\omega)$. Measurement of the high-frequency regime offers new insight into the local dynamics of actin filaments inside their tube formed by the surrounding filaments. For instance, the frequency dependence of the elastic modulus can be explained within

the framework of the model of Isambert, Maggs, and Morse (Isambert et al., 1995; Morse, manuscript submitted for publication). This model, which predicts $G^*(\omega) \propto (i\omega)^\alpha$ with $\alpha = 3/4$, assumes that at times smaller than a characteristic time τ_e, the effects of entanglements as well as the rigidity of F-actin only allow for actin filaments to fluctuate laterally. In this model, the exponent 3/4, which would become 1/2 for flexible polymers, directly reflects the finite rigidity of actin (Isambert et al., 1995; Gittes et al., 1993). Because the ratio of loss and storage moduli is related to α by $G''/G' = \tan(\alpha\pi/2) \approx 2.41$, Morse's model correctly predicts that dissipation effects dominate the viscoelastic response of F-actin networks at high frequencies (Morse, manuscript submitted for publication).

The elastic modulus has a small magnitude and a weak concentration dependence

Comparison with published data and theoretical models

Another direct effect of the finite rigidity of F-actin is the concentration dependence of the plateau modulus. Few systematic studies of the concentration dependence of the elastic plateau modulus are available. Janmey and co-workers have reported $G'_p(c) \propto c^{2.2}$ for 9.6 μM $< c <$ 24 μM with a magnitude between $G'_p \approx 150$ dynes/cm^2 and $G'_p \approx$ 1000–5000 dynes/cm^2, respectively (Janmey et al., 1988, 1990, 1991, 1994; Hvidt and Janmey, 1990). Similar magnitude and concentration dependence have been reported by other groups (Hvidt and Heller, 1990; Muller et al., 1991; Newman et al., 1993). Our mechanical and optical measurements of the amplitude of the elastic modulus, which agree with one another to within 20%, yield values that are between 15 and 200 times smaller. Our measurements are, however, in good agreement with those published by Sato et al. (1985, 1987), Wachstock et al. (1993, 1994), and Haskell et al. (1994).

Two models that specifically describe the rheology of F-actin networks have recently appeared in the literature. Isambert and Maggs (1996) and Morse (manuscript submitted for publication) assume that the small-frequency plateau modulus stems from the slow motion of the actin filaments, hindered by the surrounding cage formed by the other filaments. MacKintosh et al. (1995) postulate instead that the plateau modulus originates from the fast, hindered lateral motion of subsection of actin filaments between entanglements. These models present different predictions for the magnitude and the concentration dependence of the plateau modulus. We first test the model of Isambert, Maggs, and Morse by comparing the measured and predicted magnitudes of the elastic modulus for $c = 24$ μm. This model predicts that the plateau modulus is given by $G'_p \approx 7k_BT\rho/5l_e$, where l_e is the entanglement length, l_p is the persistence length of F-actin, and ρ is the contour length of F-actin per unit volume. Direct measurement of the entanglement length is difficult; we estimate it by using a geometric argument given in Morse (manuscript submitted for publication), $l_e \cong l_p(\rho l_p^2)^{-2/5} \approx 0.32$–$0.41$ μm with a persistence length $l_p = 5$–17 μm (Gittes et al., 1993; Isambert et al., 1995). Here, ρ is given by $\rho = cl_AN_A \cong 38.5$ μm^{-2} when $c = 24$ μM; N_A is Avogadro's number; and $l_A = 2.75$ nm is the curvilinear length of a G-actin monomer. We find $G'_p \approx 7k_BT\rho/5l_e \approx 6$ dynes/cm^2, which is slightly smaller than our measured plateau modulus. The model of Isambert, Maggs, and Morse also correctly predicts the concentration dependence of the low-frequency plateau modulus: we find $G'_p \propto c^{1.2\pm0.2}$, whereas the model predicts $G'_p \propto c^{7/5}$.

We now compare the measured concentration dependence and magnitude of the plateau modulus with the predictions of the model of MacKintosh, Käs, and Janmey (MacKintosh et al., 1995). That model predicts that the plateau modulus is given by $G'_p \cong k_BTl_p^2/\xi^2l_e^3$, where ξ is the mesh size of the F-actin network. We find $G'_p \approx 7600$ dynes/cm^2, using $\xi \approx \rho^{-1/2} = 0.15$ μm, $l_p = 17$ μm, and $l_e \approx 0.41$ μm, which is much larger than our measured value of the plateau. However, the amplitude of G'_p predicted by the model of MacKintosh, Kas, and Janmey is highly dependent on the evaluation of l_e and l_p: using the estimate of l_e based on a heuristic argument that yields an entanglement length that is about twice the tube diameter $D_e \approx 0.5$ μm (Morse, 1997), $l_e \approx 1$ μm, and a smaller persistence length $l_p = 5$ μm, we obtain $G'_p \approx 45$ dynes/cm^2, which is still too large. Therefore, unlike the Isambert-Maggs-Morse estimate of G'_p, small variations in the estimates of l_e and l_p can yield to large variations in G'_p. This disagreement worsens at actin concentrations larger than $c > 24$ μM because, according to the model of MacKintosh, Kas, and Janmey, G'_p depends strongly on concentration, $G'_p \propto c^{2.2}$.

The semiquantitative agreement between our DWS measurements and the predictions of the model of Isambert, Maggs, and Morse suggests that the origin of the viscoelasticity in an F-actin network at small frequencies is not due to the lateral fluctuations of the constitutive filaments, a mechanism evoked by the model of MacKintosh, Kas, and Janmey, but is due to the reptation-like motion of each actin filament, which is restricted by the surrounding filaments of the network.

Resolution of the discrepancy between reported values of the elastic modulus

Our measurements help resolve the large discrepancy between values of the elastic shear modulus reported in the literature. Many explanations have been offered to rationalize this discrepancy. Recently, Janmey et al. (1994) observed the extreme sensitivity of both the F-actin length and shear modulus to even small shear stresses. Therefore, they attributed the discrepancy to the effect of irreversible changes in the F-actin samples that could occur during sample loading into the rheometer or initial deformation imposed to the sample before mechanical measurements. Because, in our experiments, G-actin is polymerized in situ inside the scattering cell and because our optical measure-

ments are conducted in the linear rheological regime by definition, our measurements reject these explanations for the origin of the discrepancy.

Janmey et al. (1994) also pointed out that layers of proteins dried and denaturated by buffer evaporation at the periphery of the tools of the rheometer can also affect measurements of elastic moduli. Most of the stress generated in a fluid placed between cone and plate (or parallel plates) is contributed by the periphery; therefore, even superficial evaporation at the edge of the tools can indeed have important effects on measured F-actin rheological properties. Again, our optical measurements avoid any possible spurious effect of buffer evaporation, because the scattering cell is tightly capped after G-actin solution loading, and the laser beam is incident upon the cell at a point far away from the air-solution interface.

Implications in cell biology

The actual magnitude of the elastic shear modulus is important because a high value supports the hypothesis (Janmey et al., 1998, 1990, 1991, 1994) that isotropic F-actin networks alone are sufficiently strong to stabilize cells and provides a baseline against which to monitor subtle changes in the mechanical properties of F-actin networks due to regulating proteins, as well as small changes due to polymerization of actin filaments from ATP-containing or ADP-containing subunits (Janmey et al., 1990; Pollard et al., 1986). Our new measurements directly reject a high value for the elastic modulus and therefore the possibility that F-actin networks alone can generate the rigidity necessary for cell activities as important as cell locomotion, cell protrusion, and prevention of cell collapse. This conclusion is further supported by the observation (Janmey et al., 1994) that a mild shear flow can dramatically reduce the elastic modulus of an F-actin network, which is confirmed by our own rheological measurements in the nonlinear regime (see Fig. 9). Indeed, because cells are constantly subjected to large external and internal strains, which can be larger than 10%, F-actin networks alone cannot provide the necessary strength to prevent cell collapse. Hence, the cytoskeleton absolutely requires the combined action of F-actin and either other cytoskeletal filamentous proteins (microtubules and intermediate filaments) or actin-cross-linking proteins (α-actinin, tensin, vinculin, etc.), a conclusion reached by other authors (Wachstock et al., 1993; Condeelis, 1993, and references therein).

The authors acknowledge D. Morse, A. Maggs, and T. D. Pollard for insightful discussions. DW and SCK acknowledge financial support from the Whitaker Foundation (DW, SCK) and the National Science Foundation, grants DMR 9623972 (DW), CTS 9502810 (DW), and CTS 9625468 (DW).

REFERENCES

Casella, J. F., E. A. Barron-Casella, and M. A. Torres. 1995. Quantitation of capZ in conventional actin preparations and methods for further purification of actin. *Cell Motil. Cytoskel.* 30:164–170.

Casella, J. F., and M. A. Torres. 1994. The Cytoskeleton and Cell Function. D. Helfman, E. Raff, editors. Cold Spring Harbor Laboratory, Cold Spring Harbor, NY.

Condeelis, J. 1992. Are all pseudopods created equal? *Cell Motil. Cytoskel.* 22:1–6.

Condeelis, J. 1993. Life at the leading edge: the formation of cell protrusions. *Annu. Rev. Cell. Biol.* 9:411–444.

Coppin, C. M., and P. C. Leavis. 1993. Quantitation of liquid crystalline ordering in F-actin solutions. *Biophys. J.* 63:794–807.

Ferry, J. D. 1980. Viscoelastic Properties of Polymers. John Wiley and Sons, New York.

Gittes, F., B. Mickey, J. Nettleton, and J. Howard. 1993. Flexural rigidity of microtubules and actin filaments measured from thermal fluctuations in shape. *J. Cell Biol.* 120:923–934.

Haskell, J., J. Newman, L. A. Selden, L. L. Gershman, and J. E. Estes. 1994. Viscoelastic parameters for gelsolin length regulated actin filaments. *Biophys. J.* 66:A196.

Hvidt, S., and K. Heller. 1990. Viscoelastic properties of biological networks and gels. *In* Physical Networks: Polymers and Gels. W. Burchard and S. Ross-Murphy, editors. Elsevier, London. 195–208.

Hvidt, S., and P. A. Janmey. 1990. Elasticity and flow properties of actin gels. *Makromol. Chem. Macrom. Symp.* 39:209–213.

Isambert, H., and A. C. Maggs. 1996. Dynamics and rheology of actin solutions. *Macromolecules.* 29:1036–1042.

Isambert, H., P. Venier, A. C. Maggs, A. Fattoum, R. Kassab, D. Pantaloni, and M.-F. Carlier. 1995. Flexibility of actin filaments derived from thermal fluctuations. *J. Biol. Chem.* 270:11437–11444.

Janmey, P. A., U. Euteneuer, P. Traub, and M. Schliwa. 1991. Viscoelastic properties of vimentin compared with other filamentous biopolymer networks. *J. Cell Biol.* 113:155–160.

Janmey, P. A., S. Hvidt, J. A. Käs, D. Lerche, A. C. Maggs, E. Sackmann, M. Schliwa, and T. P. Stossel. 1994. The mechanical properties of actin gels. *J. Biol. Chem.* 269:32503–32513.

Janmey, P. A., S. Hvidt, J. Lamb, and T. P. Stossel. 1990. Resemblance of actin-binding protein/actin gels to covalently crosslinked networks. *Nature.* 345:89–92.

Janmey, P. A., S. Hvidt, J. Peetermans, J. Lamb, J. D. Ferry, and T. P. Stossel. 1988. Viscoelasticity of F-actin/gelsolin complexes. *Biochemistry.* 88:8218–8227.

Isambert, H., P. Venier, A. C. Maggs, A. Fattoum, R. Kassab, D. Pantaloni, and M.-F. Carlier. 1995. Flexibility of actin filaments derived from thermal fluctuations. *J. Biol. Chem.* 270:11437–11444.

MacKintosh, F. C., J. A. Käs, and P. A. Janmey. 1995. Elasticity of semiflexible biopolymer networks. *Phys. Rev. Lett.* 75:4425–4428.

MacLean-Fletcher, S. D., and T. D. Pollard. 1980. Viscometric analysis of the gelation of acanthamoeba extracts and purification of two gelation factors. *J. Cell. Biol.* 85:414–428.

Mason, T. G., A. Dhople, and D. Wirtz. 1997a. Concentrated DNA solution rheology and microrheology. *MRS Symp. Proc.* 463:153–158.

Mason, T. G., A. Dhople, and D. Wirtz. 1998. Linear viscoelastic moduli of concentrated DNA solutions. *Macromolecules.* 31:3600–3603.

Mason, T. G., K. Ganesan, J. V. van Zanten, D. Wirtz, and S. C. Kuo. 1997b. Particle-tracking microrheology of complex fluids. *Phys. Rev. Lett.* 79:3282–3285.

Mason, T. G., and D. Weitz. 1995. Optical measurements of frequency-dependent linear viscoelastic moduli of complex fluids. *Phys. Rev. Lett.* 74:1254–1256.

Muller, O., H. Gaub, M. Barmann, and E. Sackmann. 1991. Viscoelastic properties of sterically and chemical cross-linked actin networks in the dilute and semidilute regime: measurements by an oscillating disk rheometer. *Macromolecules.* 24:3111–3120.

Newman, J., N. Mroczka, and K. L. Schick. 1989a. Dynamic light scattering measurements of the diffusion of probes in filamentous actin solutions. *Biopolymers.* 28:655–666.

Newman, J., K. L. Schick, and K. S. Zaner. 1989b. Probe diffusion in cross-linked actin gels. *Biopolymers.* 28:1969–1980.

Newman, J., K. S. Zaner, K. L. Schick, L. C. Gershman, L. A. Selden, H. Kinosian, J. Travis, and J. E. Estes. 1993. Nucleotide exchange and rheometric studies with F-actin prepared from ATP- or ADP-monomeric actin. *Biophys. J.* 64:1559–1566.

Palmer, A., J. Xu, and D. Wirtz. 1998. High-frequency viscoelasticity of crosslinked actin filament networks measured by diffusing wave spectroscopy. *Rheologica Acta.* 37:97–106.

Petka, W. A., J. L. Harden, K. P. McGrath, D. Wirtz, and D. A. Tirrell. 1998. Reversible hydrogels from self-assembling artificial proteins. *Science.* 281:389–392.

Pollard, T. D., I. Goldberg, and W. H. Schwarz. 1986. Nucleotide exchange, structure, and mechanical properties of filaments from ATP-actin and ADP-actin. *J. Biol. Chem.* 267:20339–20345.

Sato, M., G. Leimbach, W. H. Schwarz, and T. D. Pollard. 1985. Mechanical properties of actin. *J. Biol. Chem.* 260:8585–8592.

Sato, M., W. H. Schwarz, and T. D. Pollard. 1987. Dependence of the mechanical properties of actin/α-actinin gels on deformation rate. *Nature.* 325:828–830.

Schmidt, F. G., F. Ziemann, and E. Sackmann. 1996. Shear field in actin networks by using magnetic tweezers. *Eur. Biophys. J.* 24:348–353.

Schnurr, B., F. Gittes, F. C. MacKintosh, and C. F. Schmidt. 1997a. Determining microscopic viscoelasticity in flexible and semiflexible polymer networks from thermal fluctuations. *Macromolecules.* 30: 7781–7792.

Schnurr, B., F. Gittes, P. D. Olmsted, C. F. Schmidt, and F. C. MacKintosh. 1997b. Local viscoelasticity of biopolymer solutions. *MRS Symp. Proc.* 463:15–20.

Spudich, J. A., and S. Watt. 1971. The regulation of rabbit skeletal muscle contraction. *J. Biol. Chem.* 246:4866–4871.

Wachstock, D., W. H. Schwarz, and T. D. Pollard. 1993. Affinity of α-actinin for actin determines the structure and mechanical properties of actin filament gels. *Biophys. J.* 65:205–214.

Wachstock, D., W. H. Schwarz, and T. D. Pollard. 1994. Crosslinker dynamics determine the mechanical properties of actin gels. *Biophys. J.* 66:801–809.

Weitz, D. A., and D. J. Pine. 1993. Dynamic Light Scattering. Oxford University Press, Oxford.

Xu, J., W. H. Schwarz, J. A. Käs, T. P. Stossel, P. A. Janmey, and T. D. Pollard. 1998a. Mechanical properties of actin filament networks depend on preparation, polymerization conditions, and storage of actin monomers. *Biophys. J.* 74:2731–2740.

Xu, J., D. Wirtz, and T. D. Pollard. 1998b. Crosslinker dynamics of alpha-actinin govern the mechanical properties of actin filament networks. *J. Biol. Chem.* 273:9570–9576.

Xu, J., V. Viasnoff, and D. Wirtz. 1998c. Compliance of actin filament networks measured by particle-tracking microrheology and diffusing wave spectroscopy. *Rheologica Acta*. 37:387–398.

Zaner, K. S., and T. P. Stossel. 1983. Physical basis of the rheological properties of F-actin. *J. Biol. Chem.* 258:11004–11009.

Zaner, K. S. 1986. The effect of the 540-kilodalton actin crosslinking protein, actin binding protein, on the mechanical properties of F-actin. *J. Biol. Chem.* 261:7615–7620.

Zaner, K. S., and T. P. Stossel. 1982. Some perspectives on the viscosity of actin filaments. *J. Cell. Biol.* 93:987–991.

Zaner, K. S., and J. H. Hartwig. 1988. The effect of filament shortening on the mechanical properties of gel-filtrated actin. *J. Biol. Chem.* 263: 4532–4536.